16. ELEMENTAL AND STABLE ISOTOPIC COMPOSITION OF SOME METALLIFEROUS AND PELAGIC SEDIMENTS FROM THE GALAPAGOS MOUNDS AREA, DEEP SEA DRILLING PROJECT LEG 70[1]

T. J. Barrett[2] and H. Friedrichsen, Abt. Geochemie, Mineralogisches Institut, Universität Tübingen, 7400 Tübingen, Federal Republic of Germany
and
A. J. Fleet,[3] Department of Geology, Goldsmiths' College, University of London, United Kingdom

ABSTRACT

Nontronite, the main metalliferous phase of the Galapagos mounds, occurs at subsurface depths of about 2 to 20 meters; Mn-oxide material is limited to the upper 2 meters of the mounds. The nontronite forms intervals of up to a few meters' thickness, consisting essentially of 100% nontronite granules, which alternate with intervals of normal pelagic sediment.

Electron microprobe analyses of nontronite granules from different core samples indicate that: (1) there is little difference in major element composition between nontronites from varying locations within the mounds, with adjacent granules from a given sample having very similar compositions; (2) individual granules show little internal variation in composition. This indicates that the granules are composed of a single mineral of essentially constant composition, consistent with relatively uniform conditions of Eh and composition during nontronite formation. Mn-oxide crusts have very low Fe contents, a feature characteristic of rapidly deposited Mn-oxide crusts formed under hydrothermal influences.

The rare-earth element (REE) abundances of the nontronites are generally extremely low, totalling less than several ppm. Two samples have the negatively Ce anomaly typical of authigenic precipitates formed relatively rapidly from seawater. A Mn-oxide crust sample has low REE contents, typical of Mn-oxide crusts formed under hydrothermal influences, but no negative Ce anomaly. A sample of unusual Mn–Fe-oxide mud has relatively high REE concentrations and a seawater-type pattern; both of these features are also found for metalliferous sediments from the East Pacific Rise.

The oxygen and hydrogen isotopic composition of the nontronites define a restricted field within a $\delta^{18}O$–δD plot. In manganiferous sediments, $\delta^{18}O$ and δD appear to decrease with increase in the Mn-oxide content of the sediment. From the $\delta^{18}O$ values of the nontronites, formation temperatures in the range of about 20–30°C have been estimated. By comparison, temperatures of up to 11.5°C at a 9-meter depth have been directly measured within the mounds (Corliss et al., 1979), and heat-flow data suggest present basement/sediment interface temperatures of 15–25°C. In a plot of Fe + Mn vs. $\delta^{18}O$, the Mn-oxide crust and Mn–Fe-ooze plot near the tie-lines for authigenic Mn nodules and silicate phases, implying that they have formed in isotopic equilibrium with seawater at or close to bottom-water temperatures.

INTRODUCTION

The main metalliferous component of the Galapagos mounds is nontronite, which was encountered at subsurface depths of about 2 to 20 meters in Holes 506, 507, and 509 on Leg 70 of the Deep Sea Drilling Project (DSDP). Within this depth range, nontronite intervals up to 2 to 3 meters thick, consisting essentially of 100% nontronite granules, alternate with beds of normal pelagic sediment. Gradations from granular nontronite through finer-grained compact nontronitic mud to pelagic ooze are also present. Mn-oxide crusts are confined to the upper 2 meters of the drilled mounds. Details of the stratigraphic relations are given in the individual site chapters.

In the present study, we have analyzed a suite of sediments from the Galapagos mounds area, in which are included nontronites, Mn-oxide crusts, Mn–Fe-oxide mud, and pelagic oozes. Electron-microprobe analyses of nontronite granules were carried out to determine the chemical composition of the nontronites and to ascertain whether compositional variations exist from mound to mound or from granule to granule. Concentrations of rare-earth elements (REE) and compositions of oxygen and hydrogen isotopes from the sediment suite have been measured in order to provide data for comparison with other types of sediment. The $\delta^{18}o$ composition of nontronites additionally provides an estimate of their temperature of formation.

SAMPLES

With two exceptions, the nontronite samples are granular (granules typically 2–10 mm in diameter) and were taken from sections of the core where the nontronite was homogeneous in appearance; the exceptions are from a transitional nontronitic mud layer. The four pelagic sediment samples are foraminifer nannofossil oozes containing about 5 to 10% clays and less than 10% siliceous microfossils. The Mn-oxide crust samples consisted of several hard metallic plates (up to 20 × 10 × 5 mm in size); soft black porous material about 1 mm

[1] Honnorez, J., Von Herzen, R. P., et al., *Init. Repts. DSDP*, 70: Washington (U.S. Govt. Printing Office).
[2] Present address: Department of Geology, University of Toronto, Toronto, Ontario M5S 1A1, Canada.
[3] Present address: Exploration and Production Division, British Petroleum, Research Centre, Sunbury-on-Thames, England.

thick is commonly present on one or both sides of the plates. One sample is from the middle of the main unit of Mn-oxide crust recovered, near the top of Hole 509B; this unit consisted of 1.4 meters of 100% Mn-oxide fragments. The other sample is from a 30-cm interval near the top of Hole 506C, over which Mn-oxide fragments are intermixed with nontronite granules, probably as a result of drilling disturbance. Mn–Fe-oxide mud, present only in Hole 509B, occurs as two fairly well-defined layers about 10 cm thick near the top of the hole, directly above and below the main interval of Mn-oxide crust.

ANALYTICAL TECHNIQUES

For electron microprobe analysis of the nontronites, particularly firm granules were selected and immersed in a warm resin which, after cooling, formed a hard plastic mount. The mount was then ground down until granule interiors were exposed. Mn-oxide plates were cut with a rock saw normal to their length. All samples were polished and carbon-coated in conventional fashion, then analyzed using a Cambridge Instruments Microscan 9 microprobe, at Oxford University.

Instrumental neutron-activation analysis was used to determine the abundances of up to 11 of the REE in the samples. Aliquots of the powdered samples and USGS standard rock BCR-1, of known dry weight, together with elemental standards were irradiated in the University of London Reactor at a thermal neutron flux of about 0.9×10^{12} neutrons cm^{-2} s^{-1} for 38.5 hours. After a cooling period of four days the actitities resulting from the REE were detected using a pure germanium low-energy photon detector with the following specifications: resolution (FWHM) of 550 eV at 122 keV; active volume, 300 mm^3; drift depth, 7 mm.

For X-ray diffraction analysis, samples were ground to a fine powder, then prepared as oriented mounts, using vacuum filtration. Samples were analyzed using CoK_α radiation and a scanning rate of 1°/minute.

Measurements of oxygen and hydrogen isotopes were carried out with a 60°, 15-cm single focusing mass spectrometer at the University of Tübingen. Samples weighing 20 to 30 g weight were powdered using an agate mortar and pestle and rinsed with distilled water (sample splits were used for the REE analyses). For nontronites and manganiferous samples, oxygen was extracted from whole-sediment powders using the bromine-pentafluoride procedure (Clayton and Mayeda, 1963). The method described by Godfrey (1962) was used to extract hydrogen. Compositions of oxygen and hydrogen isotopes are reported using normal δ-notation relative to SMOW (Standard Mean Ocean Water). Oxygen and carbon isotope compositions of the carbonate component of pelagic oozes are reported relative to SMOW and PDB standards, respectively. Routine reproducibility of $\delta^{18}O$, δD, and $\delta^{13}C$ values is typically 0.15‰, 2‰, and 0.05‰, respectively.

RESULTS AND DISCUSSION

Major Elements

Data for major elements are given for nontronites in Tables 1 to 3 and for Mn-oxide crusts in Table 4. Table 1 lists analyses for one of the stratigraphically shallowest nontronite layers recovered, from 3.5 meters subsurface in Hole 509B. Table 2 gives analyses for one of the stratigraphically deepest nontronite layers, from 21.5 meters subsurface in Hole 507D. The individual granules in the two samples listed in Tables 1 and 2 are typically 2 to 10 mm in diameter and represent adjacent granules formed within 3 cm of each other. Table 3 lists analyses of single large nontronite granules (6–10 mm diameter) selected from three different holes. Fe contents are expressed in terms of Fe_2O_3 because Fe^{+2} generally constitutes less than 5% of the total Fe (Donnelly, 1980; Moorby and Cronan, this volume).

The data in Tables 1 to 3 indicate that: (1) there is little difference in the major element composition between stratigraphically shallow and deep nontronites, or between nontronites from different mounds; (2) adjacent granules from a given sample of nontronite have very similar compositions; and (3) individual granules show little internal variation in composition. In particular, the Fe_2O_3/SiO_2 ratio shows only minor variation within granules and between adjacent granules. These data indicate that the analyzed granules are composed of a single mineral of essentially constant composition and do not contain any other detectable intermixed components, such as remnant biogenic tests or amorphous material. The small differences in absolute element concentrations that do exist among adjacent granules could be partly the result of variations in the content of structurally bound water. Nontronites from the mounds area typically have ignition losses of between 6 and 10% (Hoffert et al., 1980).

Table 1. Electron-microprobe analyses of adjacent nontronite granules from a stratigraphically shallow nontronite sample (Sample 509B-2-1, 44–48 cm).

Nontronite Granule	Na_2O	MgO	Al_2O_3	SiO_2	K_2O	CaO	MnO	Fe_2O_3[a]	Fe_2O_3/SiO_2	Total
Granule 1	1.07	3.64	0.02	53.27	4.27	0.35	0.04	30.91	0.580	93.57
Granule 1	1.42	3.57	0.14	52.27	4.15	0.30	0.07	30.36	0.581	92.28
Average	1.25	3.61	0.08	52.77	4.21	0.33	0.05	30.63	0.581	92.93
Granule 2	1.13	3.57	0.02	51.40	4.04	0.31	0.03	29.90	0.582	90.40
Granule 2	1.27	3.64	0.05	51.60	3.95	0.29	0.08	30.01	0.582	90.89
Average	1.20	3.61	0.04	51.50	4.00	0.30	0.06	29.96	0.582	90.65
Granule 3	1.02	3.44	0.07	52.29	4.02	0.13	0.05	31.28	0.598	92.30
Granule 3	1.21	3.67	0.26	53.86	4.45	0.18	0.07	31.55	0.586	95.25
Average	1.12	3.56	0.17	53.08	4.42	0.15	0.06	31.42	0.592	93.78
Granule 4	0.95	3.49	0.33	51.44	3.66	0.49	0.01	30.77	0.598	91.14
Granule 4	0.93	3.69	1.08	49.90	4.12	0.41	0.11	30.81	0.617	90.55
Granule 4	0.95	3.51	0.28	51.57	4.05	0.29	0.03	30.90	0.599	91.58
Granule 4	0.92	3.47	0.52	51.33	4.32	0.28	0.07	31.28	0.609	92.19
Average	0.94	3.54	0.55	51.06	4.04	0.37	0.06	30.94	0.606	91.37
1σ[b]	0.02	0.10	0.37	0.78	0.28	0.10	0.04	0.23		

[a] Total Fe as Fe_2O_3.
[b] For granule 4.

Table 2. Electron-microprobe analyses of adjacent nontronite granules from a stratigraphically deep nontronite sample (Sample 507D-6-2, 135–137 cm).

Nontronite Granule	Na_2O	MgO	Al_2O_3	SiO_2	K_2O	CaO	MnO	Fe_2O_3[a]	Fe_2O_3/SiO_2	Total
Granule 1	0.82	4.54	0.07	53.97	3.61	0.45	0.03	30.38	0.563	93.87
Granule 1	0.90	4.43	0.09	53.38	3.66	0.45	0.04	30.34	0.568	93.29
Granule 1	0.87	4.46	0.05	53.28	3.65	0.42	0.08	30.47	0.572	93.28
Average	0.86	4.47	0.07	53.54	3.64	0.44	0.05	30.40	0.568	93.48
Granule 2	0.78	4.06	0.02	50.06	3.59	0.21	0.01	27.86	0.557	86.59
Granule 2	1.52	4.03	0.05	48.69	4.03	0.11	0.01	27.23	0.559	85.66
Granule 2	1.22	4.22	0.05	49.53	3.54	0.04	0.03	26.72	0.539	85.35
Average	1.17	4.10	0.04	49.43	3.72	0.12	0.02	27.23	0.551	85.87
Granule 3	1.27	4.05	0.16	50.58	4.06	0.15	0.04	28.43	0.562	88.46
Granule 3	1.35	3.93	0.12	50.37	4.08	0.28	0.03	28.74	0.571	88.90
Average	1.31	3.99	0.14	50.48	4.07	0.22	0.04	28.59	0.567	88.68
Granule 4	0.83	4.32	0.19	55.28	3.54	n.a.	0.07	31.29	0.566	95.70
Granule 4	0.80	4.61	0.26	55.42	3.59	n.a.	0.07	31.10	0.561	95.95
Granule 4	0.84	4.69	0.23	54.95	3.65	n.a.	0.05	31.16	0.567	95.72
Granule 4	0.88	4.66	0.23	54.39	3.17	n.a.	0.07	30.59	0.562	94.13
Granule 4	0.91	4.66	0.26	52.96	3.79	n.a.	0.05	31.20	0.589	94.00
Average	0.85	4.59	0.23	54.60	3.49		0.06	31.07	0.569	95.10
1σ[b]	0.04	0.15	0.03	1.00	0.19		0.01	0.28		

[a] Total Fe as Fe_2O_3.
[b] For granule 4.

Table 3. Electron-microprobe analyses of individual nontronite granules (6–10 mm diameter) from Holes 507D and 509B.

Nontronite Granule	Na_2O	MgO	Al_2O_3	SiO_2	K_2O	CaO	MnO	Fe_2O_3[a]	Fe_2O_3/SiO_2	Total
Sample 507D-3-2, 143–145 cm										
Point A	0.34	3.51	0.16	52.18	3.66	n.a.	0.09	31.67	0.607	91.64
Point B	0.44	3.53	0.26	51.54	3.55	n.a.	0.03	31.29	0.607	90.70
Point C	0.56	0.50	0.50	51.84	2.49	n.a.	0.08	31,95	0.616	90.95
Point D	0.22	3.49	0.16	51.66	3.89	n.a.	0.07	31.66	0.613	91.19
Point E	0.06	3.70	0.23	52.77	4.03	n.a.	0.08	31.57	0.598	92.52
Point F	0.24	3.76	0.21	53.78	2.94	n.a.	0.05	32.02	0.596	93.04
Point G	0.46	3.67	0.21	52.36	2.81	n.a.	0.09	31.56	0.603	91.17
Average	0.33	3.59	0.25	52.30	3.34		0.07	31.68	0.606	91.60
1σ	0.17	0.11	0.12	0.78	0.59		0.02	0.25		
Sample 507D-6-2, 135–137 cm										
Point A	0.20	4.75	0.19	54.16	4.26	0.86	0.08	29.53	0.545	94.18
Point B	0.16	4.78	0.19	53.54	3.65	0.97	0.07	29.33	0.542	92.75
Point C	0.16	4.42	0.16	53.49	3.66	0.93	0.04	29.68	0.555	92.61
Point D	0.18	4.36	0.23	54.09	3.99	0.91	0.03	30.61	0.566	94.47
Average	0.18	4.58	0.19	53.82	3.89	0.92	0.06	29.79	0.552	93.50
1σ	0.02	0.22	0.03	0.35	0.29	0.05	0.02	0.57		
Sample 509B-2-2, 50–52 cm										
Point A	1.42	3.10	0.14	50.89	2.07	0.45	0.08	31.67	0.622	89.87
Point B	0.39	3.19	0.05	53.61	2.10	0.95	0.11	34.03	0.635	94.49
Point C	0.97	3.41	1.08	50.88	2.62	0.64	0.08	30.14	0.592	89.87
Point D	1.26	3.18	0.05	50.43	2.51	0.46	0.05	30.54	0.606	88.51
Point E	1.08	3.20	0.09	52.02	2.35	0.48	0.05	31.59	0.607	90.93
Average	1.02	3.22	0.28	51.57	2.33	0.57	0.07	31.59	0.615	90.73
1σ	0.39	0.12	0.45	1.28	0.24	0.29	0.03	1.51		

Note: n.a. = not analyzed.
[a] Total Fe as Fe_2O_3.

Data on nontronites from the Galapagos mounds area have been previously given by Corliss et al. (1978) for dredged samples and by Hekinian et al. (1978), Schrader et al. (1980), Hoffert et al. (1980), Dymond et al. (1980), and Rateev et al. (1980) for samples recovered by rotary drilling on Leg 54. These samples have major element compositions similar to the nontronites reported in this study, as do nontronites which have been recovered from the Red Sea (Bischoff, 1972), from the Gulf of Aden spreading axis (Cann et al., 1977), and from the Transform Fault Zone "A" on the Mid-Atlantic Ridge (Hoffert et al., 1978). However, there are some differences, the most notable being variations in the Fe_2O_3/SiO_2 ratio. Reported average values for this ratio range

Table 4. Electron-microprobe analyses of Mn-oxide crust fragments from Holes 507D and 509B.

Crust Fragment	Na_2O	MgO	Al_2O_3	SiO_2	K_2O	CaO	MnO	FeO[a]	Na_2O/MnO	CaO/MnO	Total
Sample 507D-2-1, 2–4 cm											
Point 1	7.31	1.00	0.21	0.08	0.74	2.42	67.07	0.36	0.109	0.036	79.50
Point 2	7.07	0.68	0.08	0.03	0.32	2.59	64.91	0.16	0.109	0.040	76.02
Point 3	7.27	1.02	0.62	1.11	0.68	2.29	66.71	0.75	0.109	0.034	80.75
Point 4	6.97	0.45	0.11	0.05	0.30	2.76	65.78	0.20	0.106	0.042	76.70
Point 5	6.68	0.60	0.27	1.43	0.49	2.34	67.10	0.34	0.100	0.035	79.50
Average	7.06	0.65	0.26	0.54	0.51	2.48	66.31	0.36	0.108	0.037	78.49
1σ	0.26	0.25	0.22	0.68	0.20	0.19	0.95	0.23	0.005	0.004	
Sample 509B-1-2, 85–90 cm											
Point 1	3.76	5.04	0.16	0.15	1.17	1.65	59.62	0.12	0.063	0.028	72.25
Point 2	3.81	4.04	0.13	0.18	1.24	1.41	62.33	0.17	0.061	0.023	73.93
Average	3.79	4.54	0.15	0.17	1.21	1.53	60.98	0.15	0.062	0.026	73.09

[a] Total Fe as FeO.

from 0.58 (Dymond et al., 1980) to 0.68 (Cann et al., 1977). The average value for the 11 separate granules analyzed in this study is 0.58.

The formation of nontronite and the evolution of the Galapagos mounds is a problem that has been discussed in detail elsewhere (Dymond et al., 1980; Hekinian et al., 1980; Honnorez, Von Herzen, et al., 1981). Briefly, the consensus of opinion is that nontronite forms primarily in response to the oxidation of reduced, basement-derived solutions as they percolate upward through the sediment column. The stratigraphic occurrence of nontronite beneath Mn-oxide crusts suggests that the oxidation profile in near-surface mounds sediments leads to the sequential precipitation of dissolved Fe^{2+} and Si as Fe^{3+}-nontronite, and then dissolved Mn^{2+} as Mn^{4+}-oxides (cf. Cann et al., 1977; Corliss et al., 1978). The near-constant composition of the nontronite granules analyzed in this study, and the apparent lack of other mineral phases intergrown within them, is consistent with relatively uniform conditions of solution Eh and composition during nontronite formation. By analogy with the experiments of Harder (1976), the solution Eh must have been relatively reducing, with a value higher than that required for Fe^{2+}-smectite formations, but lower than that required for Fe^{3+}-oxide-hydroxyoxide formation. Simultaneously, the Mg and Al contents of the solutions must have been uniformly low; otherwise compositionally different smectite minerals would have formed.

X-ray diffraction analyses have been carried out in the present study on five bulk samples from core samples apparently composed of 100% nontronite granules—that is, no other phases were visible megascopically or in smear slides. Untreated samples yielded basal (001) peaks at 12.1 to 13.4 Å, which shifted to 18.0 to 19.0 Å after glycolation (with a secondary peak at ~9.5 Å), and to 10.0 to 10.2 Å after heating at 400°C. Heating at 550°C produced no further change in the patterns except for an increase in the 10.0 to 10.2 Å peak height. These results are similar to those of Rateev et al. (1980), who reported basal peaks for untreated green-clay samples of 11.2 to 11.9 Å, which shifted to 17.8 to 18.2 Å after glycolation (with a secondary peak at 10 Å), and to 10.0 Å after heating at 550°C. These authors noted (p. 308) that because KOH saturation did not cause shifting of the basal (untreated) peak, the clay mineral was closely related to nontronite, specifically a K, Fe-smectite with mixed-layer structure in which K cations occupied some interlayer sites.

Two Mn-oxide crust samples from different Galapagos mounds have similar chemical compositions and rather high total alkali metal contents on the order of 10% (Table 4). Sample 1 has higher Na_2O but lower MgO and K_2O contents than does Sample 2. The Na_2O content of Sample 1 is in fact unusually high for mounds area Mn-oxide crusts, which consist of varying proportions of todorokite and birnessite (Corliss et al., 1978). The high Na_2O content is very unlikely to be the result of seawater contamination, for the analysis was made on a freshly cut and washed surface, and, furthermore, the sample has a near constant Na_2O/MnO ratio. Corliss et al. (1978) report Na_2O contents of up to 5.4% for Mn-oxide crusts from the Galapagos mounds. The Mn-oxide crusts are extremely low in Fe, a feature also reported for rapidly deposited Mn-oxide crusts formed under hydrothermal influences near the Galapagos spreading axis (Moore and Vogt, 1975) and in the median valley of the Mid-Atlantic Ridge (Scott et al., 1974; Toth, 1980).

Rare-Earth Elements (REE)

The REE concentrations of selected Galapagos mounds area sediments are listed in Table 5 and shown in Figures 1 and 2 together with the patterns for seawater, average lithogenic marine clay, metalliferous sediment from the east Pacific, and ferromanganese crust from the northeast Pacific. The sample numbers beside the patterns refer to the core samples listed in Table 5.

Most of the analyzed granular nontronites have extremely low REE concentrations, with total REE contents of less than several ppm; many of the REE's were below detection limits under the conditions used (Fig. 1). However, one granular nontronite (No. 4) and a sample of transitional nontronitic mud (No. 8) have seawater-type patterns, although the negative Ce anomaly of the granular nontronite is less pronounced than that

Table 5. Rare-earth element contents of metalliferous and pelagic sediments from the Galapagos mounds area, Leg 70.

Sample (No.)	Sample (interval in cm)	Lithology	La (ppm)	Ce (ppm)	Nd (ppm)	Sm (ppm)	Eu (ppm)	Gd (ppm)	Tb (ppm)	Ho (ppm)	Tm (ppm)	Yb (ppm)	Lu (ppm)
1	506-2-2, 69–71	Nontronite	2.02	b.d.	b.d.	0.38	b.d.	b.d.	b.d.	0.12	b.d.	b.d.	0.05
21	506-2-2, 132–134	Nontronite	b.d.	b.d.	b.d.	0.13	b.d.	b.d.	b.d.	b.d.	b.d.	b.d.	b.d.
3	506-4-2, 45–47	Nontronite	b.d.	b.d.	b.d.	0.08	b.d.	b.d.	b.d.	b.d.	b.d.	b.d.	b.d.
12	507D-2-1, 52–54	Nontronite	9.91	8.83	8.83	1.74	0.33	b.d.	0.27	0.61	b.d.	b.d.	0.32
23	507F-2-2, 11–13	Nontronite	1.00	b.d.	b.d.	0.16	b.d.	b.d.	b.d.	b.d.	b.d.	b.d.	b.d.
17	509B-2-1, 44–48	Nontronite	0.82	b.d.	b.d.	0.16	b.d.	b.d.	b.d.	b.d.	b.d.	b.d.	0.04
24	509B-2-2, 52–54	Nontronite	b.d.	b.d.	b.d.	0.10	b.d.	b.d.	b.d.	b.d.	b.d.	b.d.	b.d.
26	509B-3-2, 60–61	Compact nontronite	6.31	2.09	4.87	1.44	0.47	2.47	0.20	0.41	b.d.	1.27	0.19
20	509B-4-3, 37–39	Nontronite	b.d.	b.d.	b.d.	b.d.	b.d.	b.d.	b.d.	b.d.	b.d.	b.d.	b.d.
15	509B-1-2, 85–90	Mn-oxide crust	3.16	3.81	0.61	0.24	b.d.	b.d.	b.d.	b.d.	b.d.	b.d.	0.10
18	509B-2-1, 114–118	Mn–Fe oxide mud	14.0	5.95	14.4	2.75	0.54	3.75	0.49	0.90	b.d.	1.69	0.38
5	506-6-3, 39–41	Pelagic ooze	3.98	b.d.	4.12	0.69	0.26	b.d.	b.d.	0.37	b.d.	b.d.	0.09
6	506-8-1, 86–88	Pelagic ooze	4.39	4.27	4.25	0.79	0.21	b.d.	0.18	0.44	b.d.	b.d.	0.13
8	506B-2-3, 12–14	Pelagic ooze	8.21	3.47	6.99	1.35	0.30	b.d.	0.24	0.48	b.d.	b.d.	0.21
9	506B-5-1, 94–96	Pelagic ooze	8.99	15.2	11.2	0.89	0.70	b.d.	b.d.	b.d.	b.d.	1.02	0.38
Estimated detection limits:			0.51	1.88	0.55	0.07	0.12	2.03	0.05	0.11	0.63	1.00	0.02
BCR-1: This study (one determination)			22.0	60.0	24.2	5.79	1.61	8.45	0.86	1.11	b.d.	3.01	0.44
Flanagan 1973 (Recommended values)			26	53.9	29	6.6 (av.)	1.94	6.6	1.00	(1.2)	0.6	3.36 (av.)	0.55
Range of published values[a]			29–22	66–39	22–34	5.9–7.5	2.42–1.8	—	1.8–0.82	—	0.63–0.53	3.6–3.1	0.46–0.66

Note: Analysts: A. J. Fleet, S. J. Parry, and J. Thomas. b.d. = below detection *under the conditions used.*
[a] Gordon (1968); Ray et al. (1970); Flanagan (1973).

of seawater (Fig. 2). Such patterns are characteristic of phases which have formed relatively rapidly from seawater, as, for example, Fe–Mn-hydroxyoxide hydrothermal precipitates (Bender et al., 1971; Dymond et al., 1973) and Mn-oxide-rich hydrothermal crusts (Toth, 1980). REE analyses of nontronites from the Galapagos mounds by Courtois (1981), under more sensitive instrumental conditions, yielded concentrations ranging from that of Sample 4 down to values below the detection limits given in Table 5. Courtois found Ce anomalies which ranged from moderately negative (similar to pattern 4, Fig. 1) to only very slightly negative, and speculated that this range might reflect variations in the proportions of seawater-and basalt-derived REE's in the depositing solutions.

Sample 10 (Fig. 1), which consists of Mn-oxide crust, shows very low total REE contents (< 10 ppm), such as are found for rapidly formed hydrothermal Mn-oxide crusts from the TAG and FAMOUS areas of the Mid-Atlantic Ridge (Toth, 1980). The REE content of Sample 10 is far less than that of ferromanganese crusts coating basalts at midocean ridges (Fig. 1), which in turn have lower REE contents than do open-ocean Mn nodules (Toth, 1980). Sample 10, however, lacks the negative Ce anomaly typically found in Mn-oxide crusts. The REE pattern for this sample could conceivably result from a very small component of hydrogenous Mn-oxide material in the crust, since slowly forming hydrogenous Mn nodules have high REE contents (~ 1000 ppm) and pronounced positive Ce anomalies (Piper, 1973).

Sample 11 (Fig. 1) consists of Mn–Fe-oxide mud, which is present only as two 10-cm-thick layers near the top of Hole 509B. This sample has the highest concentration of REE's in the sample set and displays a seawater pattern. The pattern and the REE abundances of this sample are also very similar to those of metalliferous sediments from the East Pacific Rise (Fig. 1). This suggests that the mud might have formed by the discharge of solutions directly into seawater.

In Figure 2, the REE patterns of four pelagic oozes from the Galapagos mounds area are shown. Samples 12 and 14 have strong negative-Ce anomalies and light REE patterns, similar to that of seawater. Sample 13 has a light REE pattern similar to seawater, but with a less negative-Ce anomaly. This pattern is, however, very similar to pelagic ooze patterns from the Galapagos mounds reported by Hoffert et al. (1980). Sample 15 has an irregular pattern with only a minor negative Ce anomaly. Small admixtures (< 10%) of typical marine clays (Fig. 2) could in theory account for the reduced Ce anomalies, though in the case of Sample 15, other pattern irregularities would remain.

Composition of Oxygen and Hydrogen Isotopes

The compositions of oxygen and hydrogen isotopes of sediments from the Galapagos mounds area are listed in Table 6 and, excluding pelagic oozes, plotted in Figure 3. Sample numbers correspond to those in Table 5; a few additional samples were also analyzed.

The nontronites define a quite restricted field within the $\delta^{18}O$–δD plot and have compositions distinctly different from detrital oceanic clays (Savin and Epstein, 1970). The nontronites do not display any apparent covariation between $\delta^{18}O$ and δD. On the other hand, limited data on the Mn-oxide crust and Mn–Fe-oxide mud samples suggest that $\delta^{18}O$ and δD in manganiferous sediments both decrease with progressively higher contents of Mn oxide. (See also Fig. 4).

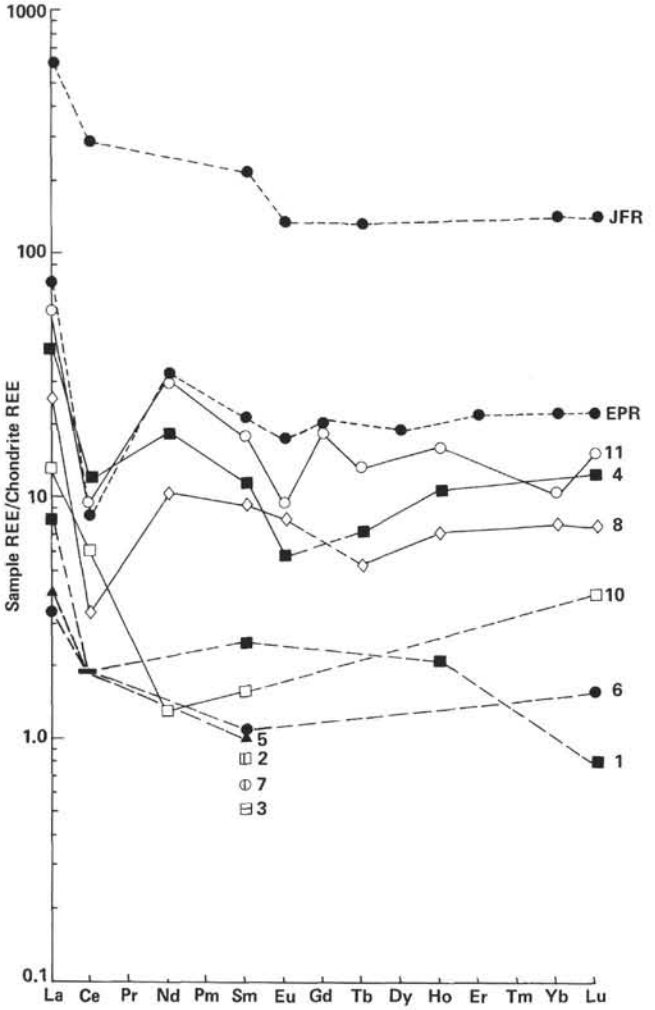

Figure 1. Chondrite-normalized rare-earth element abundances vs. atomic number for some nontronites and manganiferous material from the Galapagos mounds area, Leg 70. (Included for comparison are rare-earth element patterns for metalliferous sediment from the East Pacific Rise [E.P.R; Bender et al., 1971] and Mn–Fe crusts [average of five samples] from the Juan de Fuca Ridge in the N. E. Pacific [J.F.R; Toth, 1980]. All data have been normalized against the chondrite values of Evensen et al. [1978]. Numbers 1 to 8 are nontronites, Number 10 is Mn-oxide crust and Number 11 is a Mn–Fe-oxide mud. For Samples 1, 5, and 6, the black bar shown for Ce represents the estimated detection limits under the conditions used.)

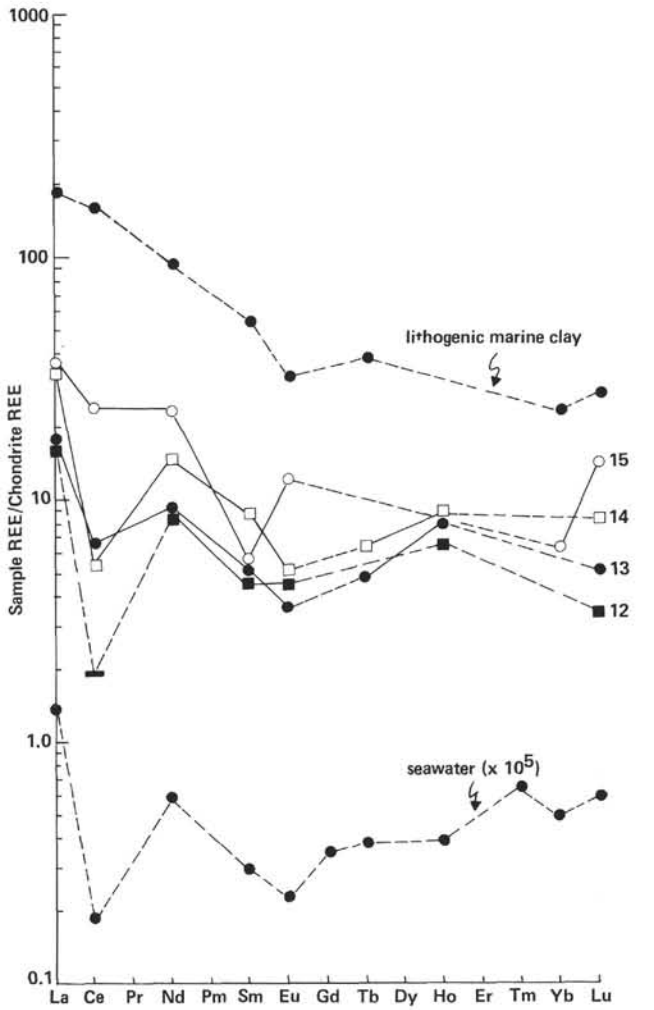

Figure 2. Chondrite-normalized rare-earth element abundances vs. atomic number for some pelagic sediments (numbers 12 to 15) Galapagos mounds area, Leg 70. (Included for comparison are rare-earth element patterns for average lithogenic marine clay [Piper, 1973] and seawater $\times 10^5$ [Høgdahl et al., 1968]. Ce bar for Sample 12 as in Figure 1. All data have been normalized against the chondrite values of Evensen et al. [1978].)

The temperatures of formation of the nontronites have been estimated from the O-isotopic composition by applying the formula of Yeh and Savin (1977) for normal smectites ($1000\ \ln\alpha = [2.67 \cdot 10^6 T^{-2}] - 4.82$). No corrections have been made for the higher Fe content of the nontronites as unpublished data of G. M. McMurtry and H.-W. Yeh (personal communications, 1981) suggest that there is no correlation between Fe content (or Mg or Al content) and $\delta^{18}O$ in a variety of authigenic marine smectites. It is assumed in these calculations that the $\delta^{18}O$ value for the solutions from which the nontronite formed was 0.0, the value for normal seawater.

The formation temperatures calculated by this method range from about 19 to 30°C for granular nontronites, and 30 to 32°C for a layer of transitional nontronitic mud (Table 6). The typical errors in $\delta^{18}O$ replicate analyses of 0.15‰ would produce a temperature-estimate error of about ±1°C. Thus, a temperature range of about 20 to 30°C can be inferred for formation of the analyzed nontronites. These values are similar to the minimum temperature values of about 30°C calculated by McMurtry and Yeh (1981) for three authigenic Fe-rich montmorillonites from surface metalliferous sediment on the crest of the East Pacific Rise and adjacent Bauer Basin (one value of 2°C was also recorded).

It is interesting to compare the estimated temperatures with directly measured temperatures reported by Corliss et al. (1979, fig. 12) from the upper portions of several Galapagos mounds. Although temperature profiles varied somewhat from mound to mound, tempera-

Table 6. Oxygen and hydrogen isotopic composition of metalliferous and pelagic sediments from the Galapagos mounds area, Leg 70, and nontronite formation temperatures as estimated from their oxygen isotope values.

Sample (No.)	Sample (interval in cm)	Lithology	$\delta^{18}O$	δD	T (°C)
1	506-2-2, 69–71	Nontronite	25.9	−135	23
21	506-2-2, 132–134	Nontronite	25.3	−124	26
3	506-4-2, 45–47	Nontronite	26.5	−120	21
5	506-6-3, 39–41	Nontronite fraction	26.0	—	23
22	506C-4-2, 74–76	Nontronite	24.9	−136	28
12	507D-2-1, 52–54	Nontronite	24.6	−122	30
23	507F-2-2, 11–13	Nontronite	26.9	−133	19
17	509B-2-1, 44–48	Nontronite	26.7	−124	20
24	509B-2-2, 52–54	Nontronite	26.2	−138	22
25	509B-3-2, 53–55	Compact nontronite	24.6	—	30
26	509B-3-2, 60–61	Compact nontronite	24.2	−124	32
20	509B-4-3, 37–39	Nontronite	26.7	−128	20
15	509B-1-2, 85–90	Mn-oxide crust	3.7	−175	
18	509B-2-1, 114–118	Mn-Fe-oxide mud	13.8	−138	
10	506C-2-1, 67–69	Mn-oxide crust	9.4	−157	
5	506-6-3, 39–41	Pelagic ooze fraction	31.8	−106	
6	506-8-1, 86–88	Pelagic ooze	32.3	−91	
8	506B-2-3, 12–14	Pelagic ooze	31.7	−99	
9	506B-5-1, 94–96	Pelagic ooze	32.6	−105	

Note: The $\delta^{18}O$ values of Samples 12, 13, 14, and 15 are for the carbonate fraction of the ooze (typically about 80%). The $\delta^{13}C$ values for these fractions are 1.5, 1.8, 0.6, and 1.9, respectively. Sample numbers correspond to those in Table 5. Numbers up to 20 also correspond to those in Table 1 of Barrett (this volume).

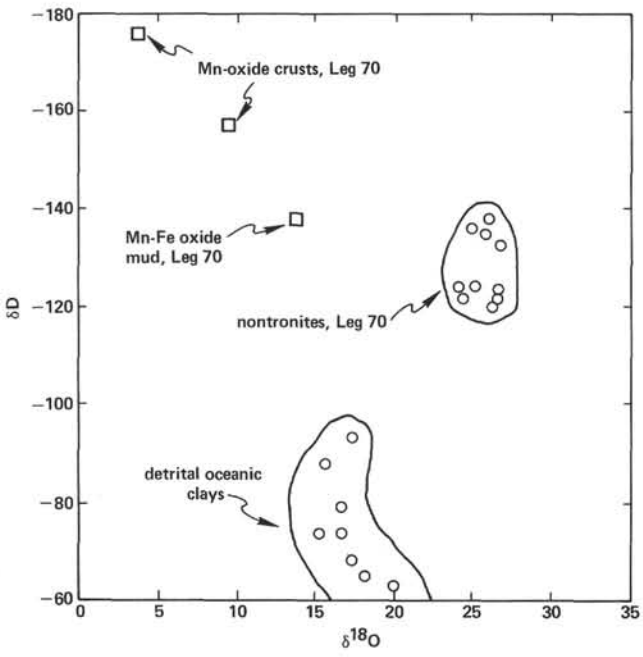

Figure 3. Plot of $\delta^{18}O$ vs. δD for some metalliferous sediments from the Galapagos mounds. (Also shown is the field of detrital oceanic clays [Savin and Epstein, 1970].)

tures increased from 2°C at the surface to 7 to 9.5°C at depths of 6 meters, and up to 11.5°C at a 9 meter depth. From their data, Corliss et al. (1979) estimated present basement/sediment interface temperatures to be about 12 to 20°C. For the mounds drilled on Leg 70, basement/sediment interface temperatures of about 15 to 20°C have been estimated on the basis of heat-flow data (Honnorez, Von Herzen, et al., 1981).

Given that the temperature range of the nontronites is about 20 to 30°C, nontronite formation therefore appears to have taken place under temperatures both overlapping with and somewhat higher than present temperatures in the mounds. This suggests that some nontronite formation may have begun when the underlying crust was closer to the spreading axis, with basement-derived solutions percolating through the sediment cover at higher temperatures than at present. It is plausible in fact that mound formation was initiated some 50,000 to 150,000 years ago, when the underlying crust was closer to the northern limit of the Galapagos mounds region (see discussion in Williams et al., 1979).

It is difficult to predict whether nontronites should yield downhole $\delta^{18}O$-temperature trends similar to those presently measured in the mounds. If nontronite formation builds up irregularly during the history of a mound, with different intervals forming at stratigraphically "random" locations and at various times (and therefore under different thermal regimes), then no regular downhole $\delta^{18}O$ temperature trend would be expected. Although no obvious trends are apparent from the data in Table 6, a much larger sample set would have to be studied before any definitive statement could be made.

It should be noted that if the solutions from which the analyzed samples formed did not have a seawater $\delta^{18}O$ value of 0.0, as assumed, but some lower value, then the calculated nontronite temperatures are maximum values. Seawater that has undergone low-temperature interactions with basalts, leading to the production of high $\delta^{18}O$ alteration phases, such as smectites, can in fact become depleted in ^{18}O (Lawrence et al., 1975). At the moment, it is unknown whether or not pore water from the mounds have been depleted by such a process.

Figure 4 illustrates the relationship between Fe + Mn and $\delta^{18}O$ given by Dymond et al. (1973) for metalliferous sediments containing varying amounts of oxide and silicate authigenic phases, and the Mn nodule–authigenic phillipsite tie-line of Savin and Epstein (1970). Also shown are the data from this study for nontronites, two Mn-oxide crusts, and the Mn–Fe oxide mud; the field of detrital oceanic clays is from Savin and Epstein (1970).

The Mn-oxide crusts and Mn–Fe-oxide mud samples plot near or on the extrapolations of the two tie-lines, implying that they formed essentially in oxygen-isotope equilibrium with seawater (Savin and Epstein, 1970), at the temperature of formation of the authigenic phases (~2°C for Mn nodules and phillipsite; Dymond et al., 1973). The nontronites, although authigenic, define a separate and distinct field. The lack of significant $\delta^{18}O$ variations is presumably the result of the rather limited variations in its temperature of formation (range of < 15°C), whereas the lack of Fe + Mn variation simply reflects the fact that nontronite is a single silicate phase with a near-constant composition.

The four pelagic sediments that were analyzed are foraminiferal nannofossil oozes (unrecrystallized), containing at least 80% calcium carbonate. The carbonate component of these sediments has $\delta^{18}O$ values ranging

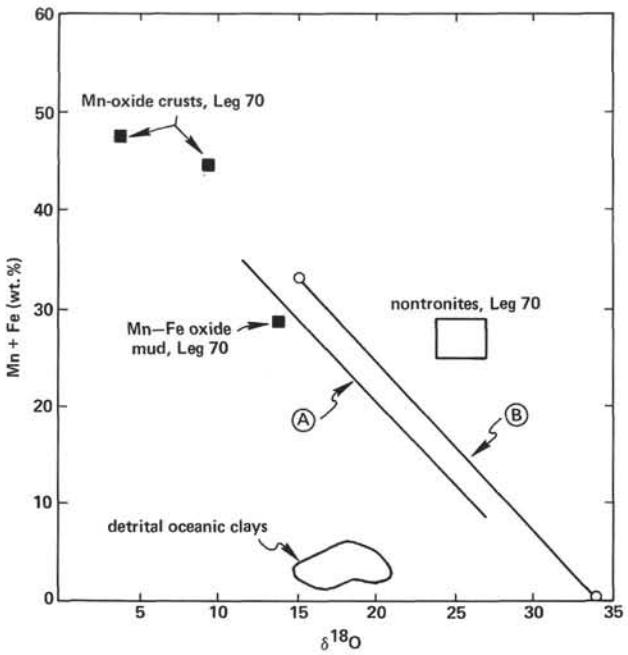

Figure 4. Plot of Fe + Mn vs. $\delta^{18}O$ for some metalliferous sediments from the Galapagos mounds. The range in Fe + Mn values shown for the nontronites is based on the data in Tables 1 to 3. The Mn + Fe values for the manganiferous sediments (Table 4 and unpublished data) are due almost entirely to the Mn component. (Also shown is the relationship given by Dymond et al. [1973] for metalliferous sediments containing varying amounts of authigenic ferromanganese and silicate phases [line A], and the authigenic Mn nodule–authigenic phillipsite tie-line [line B] of Savin and Epstein [1970]. The field of detrital oceanic sediments is from Savin and Epstein [1970].)

from 31.7 to 32.6 (Table 6). This is consistent with the occurrence of both planktonic and benthic calcareous tests in the sediments (S. Jones, pers. comm., 1981). In low latitudes, Quaternary foraminiferal and nannoplankton tests derived from warm near-surface waters have $\delta^{18}O$ values of 30 ± 0.5 ($T \doteq 17°C$), whereas benthic cold-water foraminiferal tests have values of 34 ± 0.5 ($T \doteq 2°C$) (Douglas and Savin, 1973; 1975). The measured $\delta^{18}O$ values of 31.7 to 32.6 suggest an "average" temperature for the mixed calcareous tests of 10 to 7°C (O'Neil et al., 1969). If selective dissolution of the warmer-water tests has occurred during burial of the oozes, as has been recorded elsewhere (see discussion in Douglas and Savin, 1975), then these temperatures would be somewhat lower than the average of the initially sedimented ooze. Values of $\delta^{13}C$ for the carbonate fraction, which range from 0.6 to 1.9, are also consistent with mixtures of planktonic and benthic tests (Douglas and Savin, 1973).

The δD values for the pelagic sediments (Table 6) are in the -91 to -106 range, and mainly reflect the δD values of the small percentage (< 10%) of clays present in the sediment. These δD values are somewhat lower than the δD range of detrital oceanic clays found by Savin and Epstein (1970) (Fig. 3). This could indicate that the clays in these samples partly represent alteration products derived from basaltic material. Basalts which have experienced low-temperature alteration have δD values typically in the -90 to -140 range, reflecting the formation of secondary smectites (cf. Hoernes and Friedrichsen, 1978).

ACKNOWLEDGMENTS

We are very grateful to Professor E. A. Vincent for permission to use the Oxford electron microprobe; to the director and staff of the University of London Reactor Centre for providing INAA facilities, especially to Dr. S. J. Parry for her helpful advice; to R. Curtis (Imperial College, University of London) for carrying out the XRD analyses; and to C. Fagg (Oxford University) and J. Thomas (Goldsmiths' College, University of London) for technical assistance. We also wish to thank C. Schwartz, J. Maier, and G. Bartholomä (University of Tübingen) for sample preparation and analytical assistance, and J. E. Barrett for typing the manuscript. We are grateful to Dr. J. Lawrence (Columbia University, New York) and to Dr. V. Marchig (Federal Institute for Geosciences, Hannover) for reviewing an earlier draft of the manuscript and making helpful comments. This research has been supported in part by the Natural Sciences and Engineering Research Council of Canada (T.J.B.), and by the German Science Foundation (H. F.) (D. F. G. Contract No. 357-17, 18).

REFERENCES

Bender, M., Broecker, W., Gornitz, V., Middel, U., Kay, R., Sun, S.-S., and Biscaye, P., 1971. Geochemistry of three cores from the East Pacific Rise. *Earth Planet. Sci. Lett.*, 12:425–433.

Bischoff, J. L., 1972. A ferroan nontronite from the Red Sea geothermal system. *Clays Clay Miner.*, 20:217–223.

Cann, J. R., Winter, C. K., and Pritchard, R. G., 1977. A hydrothermal deposit from the floor of the Gulf of Aden. *Mineral. Mag.*, 41:193–199.

Clayton, R. N., and Mayeda, R. K., 1963. The use of bromine pentafluoride in the extraction of oxygen from oxides and silicates for isotopic analysis. *Geochim. Cosmochim. Acta*, 27:43–52.

Corliss, J. B., Dymond, J., Gordon, L. I., Edmond, J. M., Von Herzen, R. P., Ballard, R. D., Green, K., Williams, D., Bainbridge, A. E., Crane, K., and van Andel, Tj. H., 1979. Submarine thermal springs on the Galapagos Rift. *Science*, 203:1073–1083.

Corliss, J. B., Lyle, M., Dymond, J., and Crane, K., 1978. The chemistry of hydrothermal mounds near the Galapagos Rift. *Earth Planet. Sci. Lett.*, 40:12–24.

Courtois, C., 1981. Distribution des terres rares dans les dépots hydrothermaux de la zone FAMOUS et des Galapagos—Comparaison avec les sédiments métallifères. *Mar. Geol.*, 39:1–14.

Donnelly, T. W., 1980. Secondarily modified sediments of the eastern Pacific: Major-element chemistry of Sites 420, 424, and 425, Deep Sea Drilling Project Leg 54. *In* Hekinian, R., Rosendahl, B. R.,et al., *Init. Repts. DSDP*, 54: Washington (U.S. Govt. Printing Office), 329–338.

Douglas, R. G., and Savin, S. M., 1973. Oxygen and carbon isotope analyses of Cretaceous and Tertiary Foraminifera from the central North Pacific. *In* Winterer, E. L., Ewing, J. I., et al., *Init. Repts. DSDP*, 17: Washington (U.S. Govt. Printing Office), 591–605.

_____, 1975. Oxygen and carbon isotope analyses of Tertiary and Cretaceous microfossils from the Shatsky Rise and other sites in the North Pacific Ocean. *In* Larson, R. L., Moberly, R., et al., *Init. Repts. DSDP*, 32: Washington (U.S. Govt. Printing Office), 509–520.

Dymond, J., Corliss, J. B., Cobler, R., Muratli, M., Chou, C., and Cornad, R., 1980. Composition and origin of sediments recovered by deep drilling of sediment mounds, Galapagos Spreading Center. *In* Rosendahl, B. R., Hekinian, R., et al., *Init. Repts. DSDP*, 54: Washington (U.S. Govt. Printing Office), 377–385.

Dymond, J., Corliss, J. B., Heath, G. R., Field, C. W., Dasch, E. J., and Veeh, H. H., 1973. Origin of metalliferous sediments from the Pacific Ocean. *Geol. Soc. Am. Bull.*, 84:3355–3372.

Evensen, N. M., Hamilton, P. J., and O'Nions, R. K., 1978. Rare-earth abundances in chondritic meteorites. *Geochim. Cosmochim. Acta*, 42:1199–1212.

Flanagan, F. J., 1973. 1972 values for international geochemical reference standards. *Geochim. Cosmochim. Acta*, 37:1189–1200.

Godfrey, J. D., 1962. The deuterium content of hydrous minerals from the East-Central Sierra Nevada and Yosemite National Park. *Geochim. Cosmochim. Acta*, 26:1215–1245.

Gordon, G. E., Randle, K., Goles, G. G., Corliss, J. B., Beeson, M. H., and Oxley, S. S., 1968. Instrumental activation analysis of standard rocks with high resolution γ-ray detectors. *Geochim. Cosmochim. Acta*, 32:369–396.

Harder, H., 1976. Nontronite synthesis at low temperatures. *Chem. Geol.*, 18:169–180.

Hekinian, R., Rosendahl, B. R., Cronan, D. S., Dmitriev, L., Fodor, R. V., Goll, R. M., Hoffert, M., Humphris, S. E., Mattey, D. P., Matland, J., Petersen, N., Roggenthen, W., Schrader, E. L., Srivastava, R. K., and Warren, M., 1978. Hydrothermal deposits and associated basement rock from the Galapagos spreading center. *Oceanolog. Acta*, 1:473–482.

Hekinian, R., Rosendahl, B. R., and Natland, I. H., 1980. Ocean crust geothermal processes: A perspective from the vantage of Leg 54 drilling. *In* Rosendahl, B. R., Hekinian, R., et al., *Init. Repts. DSDP*, 54: Washington (U.S. Govt. Printing Office), 395–422.

Hoernes, S., and Friedrichsen, H., 1978. $^{18}O/^{16}O$ and D/H investigations on basalts of Leg 46. *In* Dmitriev, L., Heirtzler, J., et al., *Init. Repts. DSDP*, 46: Washington (U.S. Govt. Printing Office), 253–255.

Hoffert, M. A., Perseil, A., Hekinian, R., Choukroune, P., Needham, H. D., Francheteau, J., and Le Pichon, X., 1978. Hydrothermal deposits sampled by diving saucer in transform fault "A" near 37°N on the Mid-Atlantic Ridge, FAMOUS area. *Oceanolog. Acta*, 1:72–86.

Hoffert, M., Person, A., Courtois, C., Karpoff, A. M., and Trauth, D., 1980. Sedimentology, mineralogy, and geochemistry of hydrothermal deposits from Holes 424, 424A, 424B, and 424C (Galapagos Spreading Center). *In* Rosendahl, B. R., Hekinian, R., et al., *Init. Repts. DSDP*, 54: Washington (U.S. Govt. Printing Office), 339–376.

Høghdahl, O. T., Melson, S., and Bowen, Y., 1968. Neutron activation analysis of lanthanide elements in seawater. *Adv. Chem. Ser.*, 73:308–325.

Honnorez, J., Von Herzen, R., et al., 1981. Hydrothermal mounds and young ocean crust of the Galapagos: Preliminary Deep Sea Drilling results, Leg 70. *Geol. Soc. Am. Bull.*, 92:457–472.

Lawrence, J. R., Gieskes, J. M., and Broecker, W. S., 1975. Oxygen isotope and cation composition of DSDP pore waters and alteration of layer II basalts. *Earth Planet. Sci. Lett.*, 27:1–10.

McMurtry, G. M., and Yeh, H.-W., 1981. Hydrothermal clay mineral formation of East Pacific Rise and Bauer Basin sediments. *Chem. Geol.*, 32:189–205.

Moore, W. S., and Vogt, P. R., 1975. Hydrothermal Mn crusts from two sites near the Galapagos spreading axis. *Earth Planet. Sci. Lett.*, 29:349–356.

O'Neil, J. R., Clayton, R. N., and Mayeda, T. K., 1969. Oxygen isotope fractionation in divalent metal carbonates. *J. Chem. Phys.*, 51:5547–5558.

Piper, D. T., 1973. Rare earth elements in ferromanganese nodules and other marine phases. *Geochim. Cosmochim. Acta*, 38: 1007–1022.

Rateev, M. A., Timofeev, P. P., and Rengarten, N. U., 1980. Minerals of the clay fraction in Pliocene–Quaternary sediments of the east equatorial Pacific. *In* Rosendahl, B. R., Hekinian, R., et al., *Init. Repts. DSDP*, 54: Washington (U.S. Govt. Printing Office), 307–318.

Ray, P., Wakita, H., and Schmitt, R. A., 1970. Radiochemical neutron activation analysis of indium cadmium, yttrium and 14 rare earth elements in rocks. *Anal. chim. Acta*, 51:163–178.

Savin, S. M., and Epstein, S., 1970. The oxygen and hydrogen isotope geochemistry of ocean sediments and shales. *Geochim Cosmochim. Acta*, 34:43–63.

Schrader, E. L., Furbish, W. T., Mattey, D., and May, T. A., 1980. Geochemistry and carbonate petrology of selected sediment samples from Deep Sea Drilling Project Leg 54, Eastern Pacific. *In* Rosendahl, B. R., Hekinian, R., et al., *Init. Repts. DSDP*, 54: Washington (U.S. Govt. Printing Office), 319–328.

Scott, M. R., Scott, R. B., Rona, P. A., Butler, L. W., and Nalwalk, A. J., 1974. Rapidly accumulating manganese deposit from the median valley of the Mid-Atlantic Ridge. *Geophys. Res. Lett.*, 1:355–358.

Toth, J. R., 1980. Deposition of submarine crusts in manganese and iron. *Geol. Soc. Am. Bull.*, 91:44–54.

Williams, D. L., Green, K., van Andel, Tj. H., Von Herzen, R. P., Dymond, J. R., and Crane, K., 1979. The hydrothermal mounds of the Galapagos Rift: observations with DSRV *Alvin* and detailed heat flow studies. *J. Geophys. Res.*, 84:7467–7484.

Yeh, H.-W., and Savin, S. M., 1977. Mechanism of burial metamorphism of argillaceous sediments: 3. O-isotope evidence. *Geol. Soc. Am. Bull.*, 88:1321–1330.